Lakshay Seth
Adam Glick

Dose Rate Calculation in Waveguide using Neutron Transport

Introduction:

In BNCT, a Boron-10 compound is inserted in the blood of the patient. After inserting the compound in the bloodstream, the body (tumor area) is irradiated with epithermal neutrons to yield an excited Boron-11 state, which alpha decays into Lithium-7. Thermal neutrons (energy less than 1 eV) have the highest neutron capture probability in Boron-10 (Barth, Soloway, & Brugger, 1996). The nuclear reaction is shown in Figure 1.

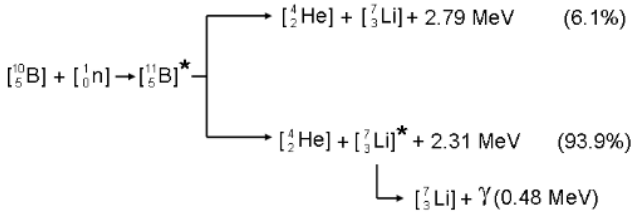

Figure 1: Nuclear Reaction of Boron-10

Since ranges of the Alpha (α) and Lithium-7 particle is 5-9 μm, equivalent to the diameter of the cell nucleus, all the energy of the reaction is released inside the tumor cell, causing considerable damage to the DNA (Sauerwein & Moss, 2009).

A problem in the BNCT application is to attain a suitabale neutron source. The neutron source can come from spalation (linear proton accelerators) or reactor cores. Each has its advantages. For spalation sources you can tune the neutron energy more easily and precisely which allows for fewer aperatures necessary in the beamline. However these sources require a lot of maintenance and take a lot of energy, causing an increase in the cost of treatment. For reactor based neutron beams there is little required in the way of maintaining the beamline. Natural sources such as these are usually maintained as the reactor core is maintained. However, in natural neutron sources the energy spectrum achieveable is much different than for spallation sources, which limits the types of treatments you can perform. An increasingly popular type of treatment is intensity modulated radiation therapy (IMRT), which modulates the dose rate and treatment field shape during beam delivery. With natural sources this is unachievable in terms of the neutron source dose rate, but can be overcome with more aperatures inbetween the beam and

the patient. For the purposes of this project, the neutron source considered will be a reactor core for a micromodular fast reactor modeled in Serpent.

Dose calculation of BNCT are complex. This is due to dose absorbed being the sum of various radiation dose components which emerge from other reactions that occur during BNCT. Along with thermal neutrons, epithermal (1 ev – 10 keV) and fast neutrons (energy greater than 10 keV) are also produced by the source (Joensuu, et al., 2003). With these neutrons available, BNCT application results in other reactions inside normal tissue. These other reactions are:

$$^{14}N + {}^{1}_{0}n \rightarrow {}^{14}C + {}^{1}_{1}p \quad (1)$$

$$^{1}H + {}^{1}_{0}n \rightarrow {}^{2}H + \gamma \quad (2)$$

$$^{1}H + {}^{1}_{0}n \rightarrow {}^{1}H + {}^{1}_{0}n \quad (3)$$

The radiation produced by these reactions is remarkably lower than level of radiation produced by the α and Lithium-7 particles.

In applications for medicine a minimum dose rate of 2 Cobalt Gray Equivalent (CGE) per minute is necessary. This is due to radiobiological effects and interplay effects of target motion and beam shape. As targets move superiorally and inferiorly they can sometimes move partially or completely out of the neutron field. This is thought to be remedied by delivering a higher dose rate so that there is less probability for tumor motion to effect the treatment.

To calculate the rudimentary dose and dose rate, an ion chamber is usually placed at a 10 cm depth in a water phantom with a neutron beam incident in a 10x10 cm square field. However, we can use empirical data and analytical models to predict what the dose rate will be by neutron interactions in water. The reason we use water is due to the similarity in neutron and photon attenuation coefficients between water and tissue. In this paper, we will be discussing the calculation of the dose rate at isocenter (100 cm from the neutron port). We will use deterministic and analytical methods to model the neutron transport in the waveguide and we will use empirical data and analytical models to calculate the dose rate at a 10 cm depth in water for a 10x10 cm neutron field.

Geometry:

The waveguide we are considering will consist of 3 main components: a capture section, a multiplying target, and a beam shaping section. In the capture section we consider a diverging trapezoidal tube with reflecting walls made from beryllium. This section diverges from the core at 30^{o} from the orthogonal plane in the radial direction and 47.9^{o} in the azimuthal direction. The

reflecting material is solid beryllium with a wall thickness of 30 cm for all four walls. In this region, outside of the reflecting material is lead-bismuth eutectic (LBE) coolant, which provides additional reflection to bring neutrons into the vacuum section; however this is not being considered in this project due to the fact that this is not a steady state system and the flow of coolant alters the reflective properties of the LBE material. This section also consists of zirconium hydride (ZrH_2) for the purpose of attenuating some of the neutrons traveling to the multiplying target. This will allow for a lower and clinically acceptable dose rate at the end of the waveguide.

The second region consists of a multiplying target made from Beryllium, where (n,2n) reactions are used to increase the neutron fluence into the shaping region. The thickness of this target is chosen to be 30 centimeters. Beryllium has a 1.7 MeV threshold (n,2n) reaction where the neutrons leaving the target carry 0.43 times the energy of the incident neutron. This will broaden the energy spectrum of our neutron fluence and allow for different aperatures to be used to shape the beam energy at the end of the waveguide. This is important for deciding what modality of neutron treatment you want to give a patient.

In the third region, the neutron beam is shaped into a 40x40 cm field using bismuth reflecting walls with thickensses of 30 centimeters. For starting conditions we consider the Washington State research reactor with BNCT room which has an orthogonal length of 0.466 meters. However because our neutron spectrum is coming from a fast reactor we choose an orthogonal length of 2 meters because scattering angles are much shallower than for those of a thermal reactor.

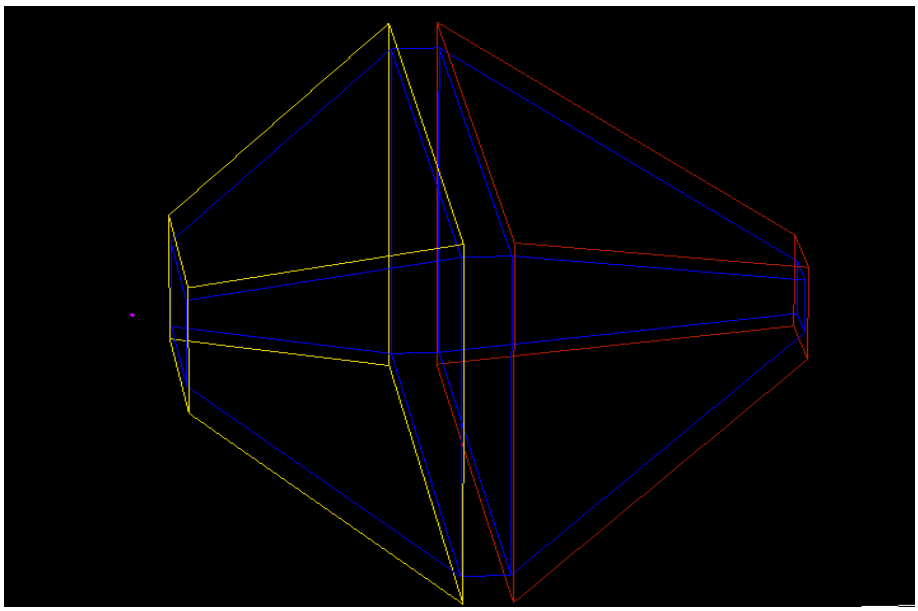

Figure 2: Geometry of waveguide generated using TOPAS MC.[10]

Mathematics:

The source of neutrons incident on our system is generated from a micro-modular fast reactor. The geometry of this reactor is a cylinder of height h = 2.4 m and radius R = 0.56 m with neutron and energy current generated from Serpent. To simplify the mathematics and geometry of the system we begin by taking the neutron current from the cylinder S_0 and transforming it to an equivalent neutron source given from an isotropic point sitting at the center of the reactor core.

(1) $S_{point} = \frac{S_0}{2\pi Rh}$

Once an isotropic point source is generated we can calculate the neutron flux incident on the waveguide as

(2) $S_{waveguide} = (S_{point} \cdot A_{waveguide})$

where

(3) $A_{waveguide} = \iint_{\theta=0,\phi=0}^{\theta=30,\phi=47.9} 4R \frac{R}{\cos(\theta)} d\theta d\phi$

This information gives the starting information we need to operate our deterministic solver. The algorithms will be discussed in the next section.

Once fluence inside the waveguide is determined, we implement the diffusion equation because neutrons have to diffuse through Zirconium(II) Hydride (ZrH_2), to get to the multiplying

material. The diffusion equation is also essential during scattering process in beryllium wall which causes the neutron to diffuse through zirconium. The diffusion equation is:

(4) $D\nabla^2\emptyset - \Sigma_a\emptyset + s = \frac{dn}{dt}$

In our case, it's time independent and can be re-written as:

(5) $\nabla^2\emptyset - \frac{1}{L^2}\emptyset + \frac{s}{D} = 0$

where L is the diffusion length

(6) $L^2 = \frac{D}{\Sigma_a}$

For our case, we determined the solution of the Differential Equation in (5) for a point source:

(7) $\emptyset(r) = \frac{Se^{-\frac{r}{L}}}{4\pi Dr}$

The source we are considering is already discretized in energy due to the output format of Serpent. From this grouping method, we discretize the particle flux in angle, where we consider 30 discretized angles that cause propagation through our reflecting material. We also consider the diffusion of particles from the source through the ZrH_2 directly but assume a completely diffusive system where scattering events remove particles from the system. Knowing the orthogonal distance from the core perimeter to the multiplying material as 1.5 meters, the distance traveled through the reflecting medium is given as

(8) $r_{Reflector} = \frac{R_{waveguide}}{\cos(\theta)\cos(\phi)}$

where $R_{waveguide}$ is the orthogonal distance of the waveguide from the reactor core to the multiplying target.

It must also be noted that to calculate the total percent of particles that scatter in the energy group traveling through the reflector we employ a similar form of (4)

(9) $N_{scatter} = N_0(1 - e^{-(\sigma_{scatter}\rho_{atomic}x)})$

While this is a valid equation for the total amount of particles that underwent scattering events, we need the differential form of this equation to give the probability density function (PDF) of the material. This provides the information on the number of particles that scattered at each step given as

(10) $dN_{scatter} = N_0\Sigma_{Be}e^{\Sigma_{Be}x}dx$

where Σ_{Be} is the macroscopic scattering cross section of Beryllium and dx is given by the intersection of the particle path with the mesh grid, which will be discussed in the next section.

We also assume total elastic scattering for ease of computation. When non-elastic events occur those particles are assumed to be removed from the system. The scattering angle is given by Fresnel's law

$$(11) \qquad (\theta', \phi') = \arccos\left(\frac{1}{n}\cos(\theta, \phi)\right)$$

$$(12) \qquad n = 1 - \frac{\lambda^2 \rho}{2\pi}$$

where ρ is the nuclear scattering length density and λ is the particle wavelength.

Combining equations (1)-(12) gives us the information needed to model the full neutron transport in the waveguide particles in the first region. Region 2 will be the neutron-multiplying phase of the geometry. This part will require information from scattering events such as angle of scatter, number of neutrons scattering at that angle, and the group energy.

To calculate the number of neutrons produced in the multiplying material, we must first calculate the nuclear cross section for (n,2n) reactions in Beryllium. This is done using linear interpolation from data taken from NNDC. After this information is calculated, we can calculate the number of neutrons produced in the multiplying target in a similar method to when we calculate the neutrons that scatter in the reflecting material. However we must keep in mind that this time we get twice as many neutrons as we put in at a maximum of half the energy.

$$(13) \qquad N_{(n,2n)} = 2 \times N_0 (1 - e^{-(\sigma_{(n,2n)} \rho_{atomic} x)})$$

where this time our distance is a function of the thickness, w, of the multiplying material

$$(14) \qquad x = \frac{w}{\cos(\theta', \phi')}$$

While the maximum energy of the scattered neutrons due to (n,2n) reactions is $E_0/2$, the average energy of the scattered neutrons, considering energy transferred to the nucleus, is

$$(15) \qquad E_{f,(n,2n)} = \frac{1}{2}\left[\frac{1}{2} + \left(\frac{A-1}{A+1}\right)^2\right] \times E_0 = 0.43 E_0$$

where A is the atomic mass of Beryllium. This averages the maximum and minimum energy of the scattered neutrons after an (n,2n) reaction. Because the neutrons leaving the multiplier have forward momentum even after the (n,2n) reactions by conservation of energy and momentum we can sum up all particles leaving and treat it as a new point source with a fan-beam spread of direction. This is a simple summation of particles over the multiplying surface that did and didn't interact, given by

(16) $$S_{fan}(E) = \frac{1}{A_{target}} \sum_x S\,(E, x)$$

After leaving the multiplying region the particles enter the third and final region where the bismuth reflecting walls converge the particles into a square beam with a 40 by 40 cm area. We use equations 5-8 again to calculate how many neutrons converge into a treatment beam. This time however we are expecting the majority of neutrons in the treatment field to come from scattering events due to the small size of the exit port. We do a three-dimensional sweep across one quadrant of the reflecting walls and track the particles that make it to the exit port. We add those to particles that travel directly to the exit port and calculate the dose rate using the fluence rate to dose rate conversion table from ICRP 21, table 4.

Algorithms:

The first procedure our code does is set up a 3-dimensional mesh grid with mesh spacing of 2.5 centimeters in each direction. This mesh grid divides up our geometry into equivalent voxels and allows us to map out the position information of where our particles interact along their trajectory. The equations for the lines that make up our boundaries are coded into the system and overlaid on top of the mesh grid. The three regions are separated along the z-axis of the grid and the origin is defined as the point source location.

The next information used to model our system is the source data generated by Serpent, a Monte Carlo toolkit used for modeling nuclear reactor cores. Serpent provides the neutron current along the perimeter of the Micro-Modular reactor discussed in the beginning of the mathematics section. The data from Serpent comes in units of a fluence rate, neutrons per second and is discretized in energy bins of 0.1 MeV. After extracting the data from Serpent, our code transforms our source into an equivalent point source with units of neutrons/(cm^2s).

Using equation (10) we define the probability density function (PDF) of the boundary inside the waveguide. Due to symmetry, we only need to model one quarter of the system so we arbitrarily choose the second quadrant to model. We separate the diffuse system from the reflective system and solve them independently. We then discretize the angles in the reflective system into 6 pointing angles and 6 sweep angles. The pointing angles go from 30^o to 43.3^o in the radial direction and 42^o to 47.7^o in the azimuthal direction. These are the angles cover every direction a particle could interact with the boundary and are calculated using geometry and the fact that the boundary is 30 cm thick. The sweep angles then go from 0^o to 47.7^o in the radial direction and 0^o to 43.3^o in the azimuthal direction. These sweep angles cover the entire plane

occupied by the boundary at the pointing angle, giving the system its three-dimensional geometry.

The differential distance in equation (10) is taken to be the distance through one voxel in the mesh grid that a particle would travel along its trajectory defined by the pointing and sweep angles. The differential path length calculation starts at the intersection of the particle with the first boundary wall and stops at the intersection of the particle with the second boundary wall. Given that each voxel is 2.5 cm by 2.5 cm by 2.5 cm in dimension we can convert the path length through the voxel into a distance, dx. Our code figures out the ray that the particle will be moving along based on the incident and sweep angles it is running through and from there it determines when the particles cross into the first boundary, which gives the start of our collision path of interests and when they cross the second boundary, which gives the end point of the particle collision path. From this we calculate a dx value for every mesh voxel using the x, y, and z coordinates of the particle trajectory through two sides of each voxel between the two boundaries. We also use equation (10) to calculate the number of particles that interact via inelastic interactions and are removed from the system. For every interaction type, we subtract out that many particles from the initial particle fluence going into the next mesh voxel. We also record the scattering angle, calculated by equations (11) and (12), to determine if the particles that scattered will reach the multiplying target and what the distance through the multiplying target will be if they do. This is done for every pointing and every sweep angle in the radial and azimuthal directions in this quadrant. Sweeping through more angles and creating a finer mesh will increase the accuracy but also increase computation time.

Once particles that scattered off the reflecting walls, we use equations (6) and (7) for determining the number of particles that diffuse through ZrH_2 attenuator, followed by calculating the number of particles that are generated in the multiplication region. The path through the multiplication region is scaled based on the angle of the incoming neutrons. These angles are taken from equations (11) and (12) for scattered particles in the energy group we are looking at. We also save the angles of trajectory for particles diffusing through the system bounded by the reflecting walls. For each angle of trajectory, we use equations (13) and (14) to determine how many particles are entering the third region due to an (n,2n) reaction and equation (15) to determine the energy of those particles leaving the system. We also use a form of equation (9) with the total macroscopic cross section value minus the (n,2n) value to determine how many

particles are attenuated in the multiplier and leave the system. All other particles are considered to have not interacted and therefore have the same energy as they did entering the multiplier. Then, for reasons explained in the previous section, we use equation (16) to create two new point sources for the two groups of particles leaving the multiplier. These sources are placed at the center of the outlet side of the multiplying region.

After we have our two point sources we go through the same process as in the first region, except this time instead of verifying that the particles that scatter hit a large multiplying target, we are verifying that they particles reach a small 40 cm by 40 cm square outlet. We use the sweeping technique discussed in the first region except this time our region is 200 centimeters long to increase the probability of particles to reach the outlet. With this geometry, we go from 11.31^{o} to 90^{o} along the waveguide walls. We then sweep through 0^{o} to 49.49^{o} along the radial plane and 0^{o} to 58.66^{o} in the azimuthal plane to cover the entire geometry of the third region. As in the first region we use equation (10) to define the PDF of the boundary, which here is made of bismuth. We define a new meshgrid in this region with the same 2.5 cm spacing as the one we had created at the start of the code to create the dx values for the neutron path inside the reflecting walls of this region. The process here is the same as in the first region except for the angles we are working at and the equations of the lines that form our waveguides have a proportionally negative, and different magnitude, slope.

Code Use:

To run this code, you need to run the main function:

```
main(EnergyFlux, FluxSource, File1, File2, File3, File4, File5, File6)
```

Here is an example with our input files:

```
main('DETSurfOutNewE.txt', 'DETSurfOutNewF.txt', 'sigBe.txt',
'sigBeInelastic.txt', 'sigBi.txt', 'sigBiInelastic.txt', 'n2nBe.txt',
'D_M_n2n.txt')
```

- Input1: EnergyFlux: This file contains energy of the particles coming out of the source in MeV. These values are taken from Serpent. See Appendix [1]
- Input2: FluxSource: This filed contains flux of the particles from the source. These values are taken from Serpent. See Appendix [2]
- Input3: File1: Data in text file contains the energy in eV and corresponding cross section in barns of the reflecting material in region 1. If a different material needs to be used in

region 1, this data file along with File2 would need to be changed. For our calculations, we used Beryllium.

- Input4: File2: Data in text file contains information about inelastic scattering energy in eV and corresponding cross section in barns of the reflecting material in region 1.
- Input5: File3: Data in text file contains the energy in eV and corresponding cross section in barns of the reflecting material in region 3. If a different material needs to be used in region 3, this data file along with File4 would need to be changed. For our calculations, we used Bismuth.
- Input6: File4: Data in text file contains information about inelastic scattering energy in eV and corresponding cross section in barns of the reflecting material in region 3.
- Input7: File5: Data in the text file contains tabular data of Energy and Cross-Sections of the multiplying target which in our case is Beryllium. Energy is in units of eV and Cross-section is in barns.
- Input8: File6: Data in this text file should have two columns: ρ in $\frac{kg}{m^3}$ and molar mass (MM) in $\frac{kg}{mol}$ of the multiplying target which in our case was Beryllium.

Running the main function will output two files in the same directory. First, will be totalDoseRate.txt which will contain the total Dose Rate in Gray/min. Second will be a doserate.csv file which will contain dose rate associated with each energy.

Test Problems and Results:

The code written for this project is specific to the geometry defined above and shown in Figure 2. Our test problem comes from a micro-modular reactor core that defines what our source is. We chose to sweep through 36 total angles in the azimuthal, radial, and incident directions for region one and region three when modeling the neutron transport through the waveguide. Our results, shown in figure 3, give a total dose rate of 64.24 Gray per minute (Gy/min).

The source inputs for our test problem are given in Appendix [1] and [2] and all values for nuclear cross sections are taken from the National Nuclear Data Center (NNDC) Evaluated Nuclear Data File Library.[9] As mentioned in Code Use, the material used for each waveguide can easily be changed by simply changing the input file used for the material in that region.

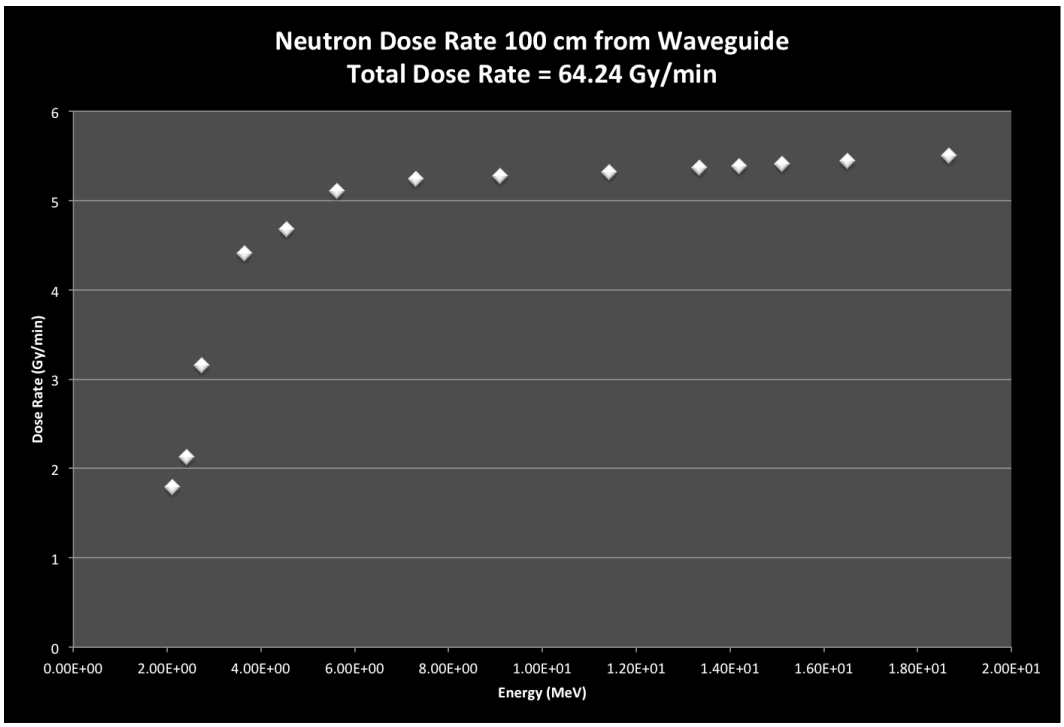

Figure 3: Results calculated by modeling neutron transport through the waveguide.

One caveat to these results is that they can be improved in accuracy by modifying the angles swept through and the grid size. We ran our code with 4, 9, and 36 total angles to verify that by including more angles we get an increase in our final value for dose rate, which was the case. Ideally, we would like to include many more angles, but for every increase in the number of angles we have the calculation time increases as well. This is also the case for the mesh grid we use. We used a 2.5-centimeter grid spacing for this project, but creating a smaller spacing such as a millimeter will increase the accuracy of the results but also will increase computation time.

Because these results are unique to the geometry we modeled there is no way to verify the code against a benchmark. What we did do was verify that we hard particle equilibrium. That is to say we checked at the end of every region if our total number of particles added up to the input. This check was to make sure we were not losing any information along the way of our calculation.

While we could not do a Monte Carlo simulation for this geometry due to time constraints, we were able to access results for a similar geometry ran in TOPAS MC for the same source information that comes close to what we calculated for our geometry. This comparison is simply a sanity check to make sure our code doesn't come up with a completely wrong answer.

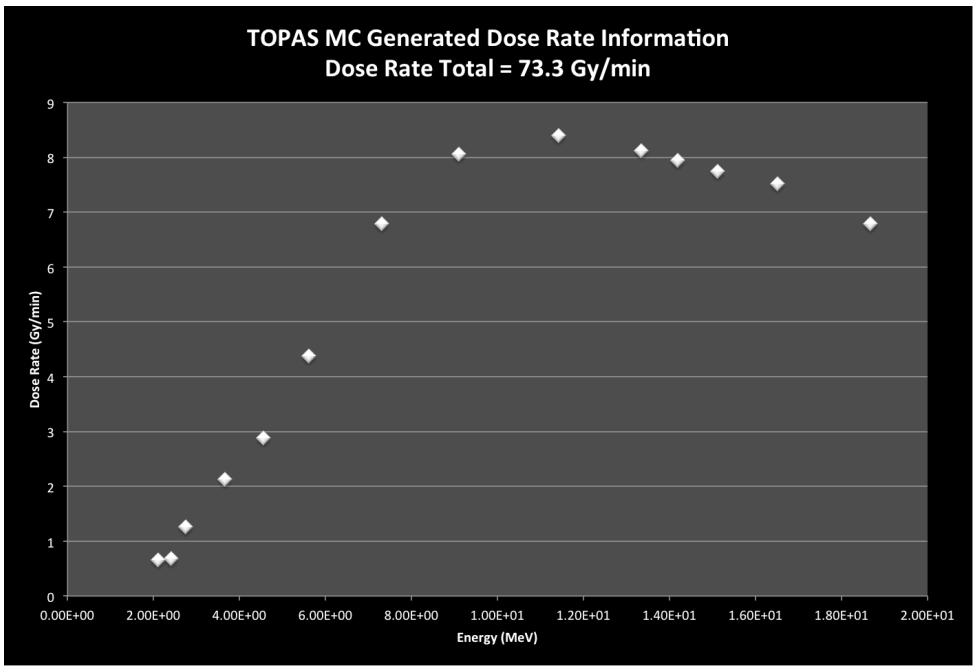

Figure 4: Results for a waveguide with similar geometry and same source generated in TOPAS MC. [10]

Summary:

We have designed a program that calculates the neutron dose rate that is expected at the isocenter of a reactor based at the neutron treatment facility. This code is designed to run for this specific geometry. It is designed to calculate the dose rate at the end of the waveguide, providing us with the information about the output of a nuclear reactor core, and whether it is optimal for therapeutic uses. It is significantly faster than Monte Carlo methods while providing a reasonably close answer. By utilizing a set of hybrid Monte Carlo-Deterministic algorithms we have created a quick and accurate method for modeling the neutron transport through this waveguide.

We can improve our results by increasing the number of incident and sweep angles and decreasing the size of the meshgrid used. For every improvement in accuracy, the code written for this project will take more time to run. The code written has also been created such that it is easy to change the source input and the materials used for each waveguide.

The final dose rate calculated for this geometry was 64.24 Gy/min. This is not a clinically acceptable dose rate as is, but adding ZrH_2 into the third region of the waveguide can decrease it. This would require additional modification to our code to include diffusion through the material, which will increase run time.

Appendix:

[1] Neutron Fluence Information Taken from Serpent

223	223	1	1	1	1	1	1	1	1	-7.22018E+15 0.00804
224	224	1	1	1	1	1	1	1	1	-1.99597E+16 0.00525
225	225	1	1	1	1	1	1	1	1	-1.88529E+16 0.00529
226	226	1	1	1	1	1	1	1	1	-3.63562E+15 0.01106
227	227	1	1	1	1	1	1	1	1	-1.14108E+16 0.00683
228	228	1	1	1	1	1	1	1	1	-1.47586E+16 0.00596
229	229	1	1	1	1	1	1	1	1	-2.85831E+15 0.01331
230	230	1	1	1	1	1	1	1	1	-4.86931E+15 0.00997
231	231	1	1	1	1	1	1	1	1	-1.61320E+15 0.01628
232	232	1	1	1	1	1	1	1	1	-4.37110E+14 0.03405
233	233	1	1	1	1	1	1	1	1	-1.32117E+14 0.05897
234	234	1	1	1	1	1	1	1	1	-8.65956E+12 0.23734
235	235	1	1	1	1	1	1	1	1	-4.53082E+12 0.31347
236	236	1	1	1	1	1	1	1	1	-1.36228E+12 0.57634
237	237	1	1	1	1	1	1	1	1	-4.51493E+11 1.00000
238	238	1	1	1	1	1	1	1	1	-4.61228E+11 1.00000

[2] Neutron Energy Information Taken from Serpent in MeV where the third column is the energy we take for our code.

1.01000E+00	1.10000E+00	1.05500E+00
1.10000E+00	1.20000E+00	1.15000E+00
1.20000E+00	1.25000E+00	1.22500E+00
1.25000E+00	1.31700E+00	1.28350E+00
1.31700E+00	1.35600E+00	1.33650E+00
1.35600E+00	1.40000E+00	1.37800E+00
1.40000E+00	1.50000E+00	1.45000E+00
1.50000E+00	1.85000E+00	1.67500E+00
1.85000E+00	2.35400E+00	2.10200E+00
2.35400E+00	2.47900E+00	2.41650E+00
2.47900E+00	3.00000E+00	2.73950E+00
3.00000E+00	4.30400E+00	3.65200E+00
4.30400E+00	4.80000E+00	4.55200E+00
4.80000E+00	6.43400E+00	5.61700E+00
6.43400E+00	8.18730E+00	7.31065E+00
8.18730E+00	1.00000E+01	9.09365E+00
1.00000E+01	1.28400E+01	1.14200E+01
1.28400E+01	1.38400E+01	1.33400E+01
1.38400E+01	1.45500E+01	1.41950E+01
1.45500E+01	1.56830E+01	1.51165E+01
1.56830E+01	1.73330E+01	1.65080E+01
1.73330E+01	2.00000E+01	1.86665E+01

References:

[1] AUTERINEN, IIRO; SALMENHAARA, SEPPO. 2005. Fir 1 Reactor in service for boron neutron capture therapy (BNCT) and isotope production. STI/PUB/1212. IAEA, ss. 313 - 324. Research Reactor Utilization, Safety, Decommissioning, Fuel and Waste Management. Proceedings Papers and Posters of an International Conference. Santiago, 10-14 Nov. 2003.

[2] Barth, Rolf F., Albert H. Soloway, and Robert M. Brugger. "Boron Neutron Capture Therapy of Brain Tumors: Past History, Current Status, and Future Potential." *Cancer Investigation* 14.6 (1996): 534-50. Web. 1 Nov. 2016

[3] CURRENT STATUS OF NEUTRON CAPTURE THERAPY, IAEA, VIENNA, 2001, IAEA-TECDOC-1223, ISSN 1011–4289

[4] Data for Protection Against Ionizing from External Sources - Supplement to ICRP Publication 15. ICRP Publication 21. 1973.

[5] Harling, Otto K. "Fission Reactor Based Epithermal Neutron Irradiation Facilities for Routine Clinical Application in BNCT—Hatanaka Memorial Lecture." *Applied Radiation and Isotopes* 67.7-8 (2009): S7-S11. Web. 20 Oct. 2016

[6] Harling, O; Riley, K., "Fission reactor neutron sources for neutron capture therapy - a critical review", Journal of Neuro-Oncology 62: 7-17, 2003.

[7] Hickey, Michelle J., Colin C. Malone, Kate L. Erickson, Martin R. Jadus, Robert M. Prins, Linda M. Liau, and Carol A. Kruse. "Cellular and Vaccine Therapeutic Approaches for Gliomas." *Journal of Translational Medicine J Transl Med* 8.1 (2010): 100. Web. 8 Nov. 2016.

[8] Joensuu, H. et al, "Boron neutron capture therapy for brain tumors: clinical trials at the Finnish facility using boronophenylalanine", *Journal of Neuro-Oncology*, 62: 123–134, 2003.

[9] National Nuclear Data Center, *Evaluated Nuclear Data File B-VII.1 Library*, http://www.nndc.bnl.gov/sigma/

[10] Perl J, Shin J, Schumann J, Faddegon B, Paganetti H. TOPAS: an innovative proton Monte Carlo platform for research and clinical applications. Med Phys. 2012 Nov; 39(11):6818-37.

[11] Sauerwein, Wolfgang A. G., and Ray Moss. "Requirements for Boron Neutron Capture Therapy (BNCT) at a Nuclear Research Reactor." *Neutron Capture Therapy* (2009): 5+. Web. 05 Nov. 2016.

[12] Slaybaugh, Rachel. *NE 255 Section 08 Notes, Monte Carlo*,

https://github.com/rachelslaybaugh/NE255/tree/gh-pages/08-monte-carlo

[13] User Guide for TOPAS Version 3.0, http://www.topasmc.org/user-guide

[14] Utsunomiya, H et al. “Photoneutron cross sections for nuclear astrophysics”, *Journal of Nuclear Science and Technology*, 39:sup2, 542-545, DOI: 10.1080/00223131.2002.10875158

Software Used:
[1] MATLAB
[2] TOPAS MC (http://www.topasmc.org/home)